Changes in the oxidation state of transition metal containing MCM-41 during deNO$_x$ reactions

A. Jentys *, W. Schießer and H. Vinek

Institute for Physical Chemistry, Technical University of Vienna, Gertreidemarkt 9/156, A-1060 Wien, Austria

Received 9 May 1997; accepted 15 July 1997

The oxidation state of Co, Pt and Rh containing MCM-41 after co-adsorption of NO, CH_4, and O_2 in the presence of water vapor was studied by in situ XANES experiments. All catalysts were oxidized after the adsorption of NO and reduced after the co-adsorption of NO and CH_4. The presence of water vapor did not influence the oxidation/reduction of Rh/MCM-41 and Pt/MCM-41, while Co/MCM-41 was oxidized by the presence of H_2O at reaction temperature.

Keywords: Co/MCM-41, Pt/MCM-41, Rh/MCM-41, in situ XANES, deNO$_x$ catalysis

1. Introduction

Nitrogen oxides are among the major air pollutants in the lower atmosphere evolving from energy conversion processes today, the main sources being the oxidation of the nitrogen from air during combustion processes and the oxidation of the nitrogen containing components of fossil fuels [1]. The catalytic reduction of NO_x with NH_3 over TiO_2/V_2O_5-based catalysts is currently the best available technology for combustion processes [2]. However, there are certain limitations of this process, e.g. the use of NH_3, which have spurred the search for alternative reactants and catalysts. Currently the main focus is oriented towards transition metal containing zeolites, which proved to be very active for deNO$_x$ reactions using hydrocarbons as reducing agents [3,4] and for decomposing NO [5]. The most active catalysts for the reduction of NO_x with hydrocarbons are Cu/ZSM5 [3] and Co/ZSM5 [6]. These materials showed almost 100% conversion at temperatures around 673 K with high selectivities towards N_2 and O_2 formation; however, the high activities are immediately reduced when water vapor is present in the gas stream [7]. Recently, it was reported that Fe/ZSM5 is highly active for the catalytic reduction of NO_x with isobutane and that the catalytic properties of this material were not retarded by the presence of H_2O and SO_2 in the reactant gas stream [8].

To understand better the influence of water on the activity of the deNO$_x$ catalysts, the oxidation state of metal clusters in MCM-41 type molecular sieves during the co-adsorption of NO, CH_4 and O_2 with and without the presence of water vapor was investigated by in situ XANES experiments. This method allows one to follow changes in the chemical state of the metal under reaction conditions and is applicable for studying the deNO$_x$ reaction without limitations of pressure and temperature [9,10].

* To whom correspondence should be addressed.

2. Experimental

2.1. Materials

MCM-41 was prepared by hydrothermal synthesis using hexadecyltrimethylammoniumbromide (C_{16} TMABr) as template [11]. After drying the samples for 72 h in air, the template was removed by heating the material in nitrogen to 813 K (heating rate 1 K min^{-1}) and maintaining it at that temperature for 2 h in nitrogen and subsequently for 8 h in dry air. The structural properties of MCM-41 were verified by XRD and N_2 sorption experiments. The pore diameter calculated from the (100) reflection in the XRD was 3.7 nm and the BET surface area was ~ 1100 m^2 g^{-1}.

The molecular sieve was loaded with 1 mol% Co, Pt or Rh by impregnation in aqueous solution. The amount of solution was chosen in such a way that the liquid was just filling up the pores of the mesoporous support. After impregnation the catalysts were dried at 343 K and calcined at 773 K in dry air.

2.2. X-ray absorption spectroscopy

The X-ray absorption spectra were measured at the SRS (Synchrotron Radiation Source, Daresbury, UK) at the beamlines 8.1 and 9.2 in transmission mode using ionization chambers filled with mixtures of He and Ar to give a $\Delta\mu x$ of 20% in the first and of 80% in the second chamber. To avoid the effects of the higher harmonics being present in the X-ray beam, the monochromator

was detuned to 50% intensity for the experiments at the Co edge and to 70% intensity on the Pt and Rh edges.

The catalysts were pressed into self-supporting wafers and placed inside a stainless-steel cell that permitted collection of the spectra in situ during the reaction. The weight of the samples was selected to achieve an absorption of less than $\mu x = 2.5$ for the reduced catalysts to optimize the signal to noise ratio and to avoid non-linear variations of μx induced by the thickness of the pellet [12].

Before each adsorption/reaction experiment the catalysts were reduced in H_2 at 873 K for 30 min and after cooling to liquid nitrogen temperature an X-ray absorption spectrum was recorded. Subsequently the catalysts were heated in He to 673 K, where all reaction experiments were carried out. The different reactants (H_2, NO, O_2, CH_4) were taken from gas cylinders and were individually mixed into the He carrier gas stream. Water was added into the gas stream using a saturator, which was kept at 298 K. The flow of all reactants was controlled by flow meters; their concentrations used are summarized in table 1. During the adsorption X-ray absorption spectra were recorded with a time resolution between 200 and 400 s.

The position of the absorption edge was determined at the maximum of the first derivative and aligned with the edge of the corresponding bulk metal. A third-order polynomial function was used to approximate the variation of the total absorption coefficient due to the background scattering. The scattering of the edge metal was calculated from the Victoreen coefficients up to 500 eV above the edge [13]. The XANES were normalized to the mass areal loading, representing the product of metal concentration and sample thickness [14]. To estimate the area of the peak above the absorption edge the continuum step was modeled by an arctan function [15]. The inflection point of this function was positioned at the half height of the absorption edge. The height of the modeled step was aligned to the spectral region starting 40 eV above the edge and the intrinsic width was obtained by adjusting the model function to the shape of the absorption edge of the corresponding bulk metal. The step function was subtracted from the XANES and the resulting peak was integrated numerically. An example of the simulation of the continuum step is shown in figure 1.

EXAFS analysis was carried out using standard anal-

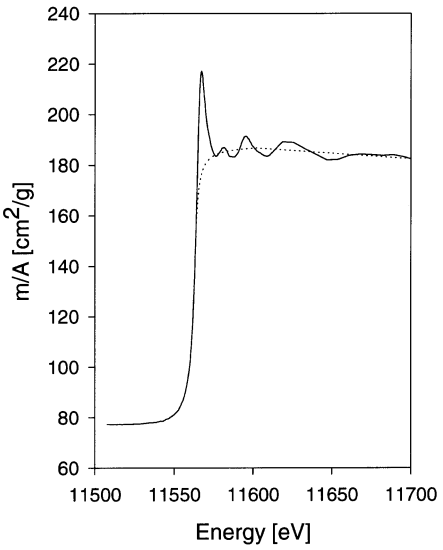

Figure 1. Simulation of the continuum step for XANES analysis.

ysis procedures as described, e.g., in refs. [16,17]. The background was removed by using a polynomial function for the baseline and the contributions of the first coordination shell were isolated by a Fourier transformation of the k^2-weighted oscillations (k = 3–16 Å^{-1}). The structural parameters were determined under the assumption of single scattering and plane waves using phase shift and amplitude functions obtained experimentally from the corresponding bulk metals.

3. Results

The results of the EXAFS analysis of the reduced samples are summarized in table 2. For Co/MCM-41 and Pt/MCM-41 a similar number of nearest neighbors was observed, while for Rh/MCM-41 this number was significantly lower. Assuming cuboctahedrally shaped particles, the average cluster sizes for Co/MCM-41 and for Pt/MCM-41 were about 60 metal atoms and for Rh/MCM-41 about 10 metal atoms [18]. Note that changes in the particle sizes after the adsorption/reaction were not observed in the EXAFS, therefore, we could assign the variations in the XANES entirely to changes of the oxidation state of the metal [19]. However, for the investigation of the sintering behavior of the metal particles the time at reaction temperature (2–3 h) was too short.

Table 1
Concentration of reactants during the experiments

Reactant	Concentration (balance He)
NO	3000 ppm
CH_4	4 vol%
O_2	10 vol%
H_2O	2.5 vol%

Table 2
Results of the EXAFS analysis of the reduced samples

Sample	Me (wt%)	N_{Me-Me}	r_{Me-Me} (Å)	$\Delta\sigma^2_{Me-Me}$ (Å^2)
Co/MCM-41	1.0	8.4	2.56	2.2×10^{-4}
Pt/MCM-41	3.2	7.9	2.78	3.5×10^{-4}
Rh/MCM-41	1.7	4.2	2.68	1.2×10^{-4}

The XANES during adsorption of 3000 ppm NO at 673 K on Rh/MCM-41 as a function of time are shown in figure 2. The changes in the area of the peak above the absorption edge during adsorption of NO with and without the presence of H_2O are compared in figure 3a for Rh/MCM-41 and in figure 3b for Pt/MCM-41, respectively. The XANES of Co/MCM-41 after adsorption of NO, H_2O and after co-adsorption of NO and H_2O together with that of bulk Co are shown in figure 4.

During adsorption of NO on transition metal containing MCM-41 the intensity of the peak above the edge increased. For Rh/MCM-41 and for Pt/MCM-41, independently of the presence of water, the same increase of the area of the peak above the edge was observed; however, the time needed to reach the partially oxidized state was significantly shorter when water was present. In contrast, Co/MCM-41 was fully oxidized after the adsorption of H_2O only and the co-adsorption of NO and H_2O on this sample led to a further increase of the oxidation state compared to the adsorption of NO.

The XANES after reduction, after adsorption of NO and after co-adsorption of NO and CH_4 with and without H_2O and of the corresponding bulk metal are shown in figure 5 for Rh/MCM-41, in figure 6 for Pt/MCM-41 and in figure 7 for Co/MCM-41. The addition of 4 vol% CH_4 into the carrier gas led to a complete reduction of Rh/MCM-41 and Pt/MCM-41, independently if H_2O was present or not. In contrast, Co/MCM-41 was only slightly reduced when CH_4 was added into the reaction gas mixture, but similar to the other samples, the oxidation state was independent of the presence of H_2O vapor.

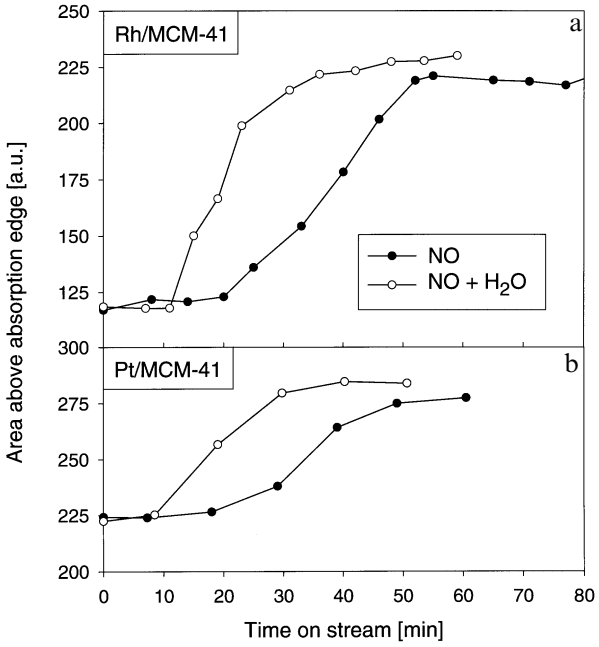

Figure 3. Changes in the area of the peak above the absorption edge during adsorption of NO with and without the presence of H_2O (a) Rh/MCM-41, (b) Pt/MCM-41.

Note that during these experiments 3000 ppm of NO were present in the reaction gas.

For Pt and Rh the XANES of the metal foils was almost identical to that of the reduced catalysts, while for Co a slight increase of the peak above the edge was observed for the reduced Co/MCM-41 sample compared to the bulk metal. We already observed this difference for Co and Ni containing ZSM5 zeolites [20] and have assigned them either to the presence of small con-

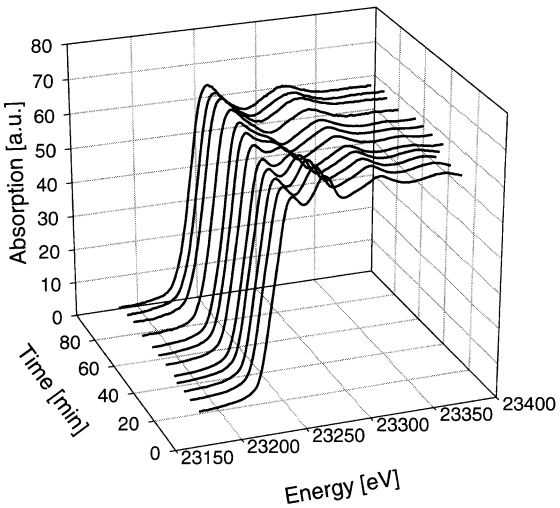

Figure 2. Time-resolved XANES during adsorption of 3000 ppm NO at 673 K on Rh/MCM-41.

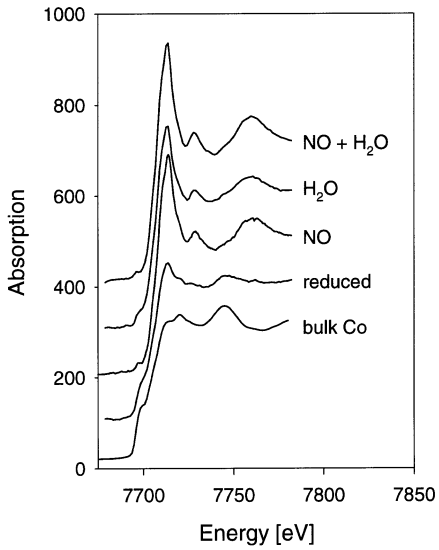

Figure 4. XANES of Co/MCM-41 after adsorption of NO, H_2O, after co-adsorption of NO and H_2O and of bulk Co.

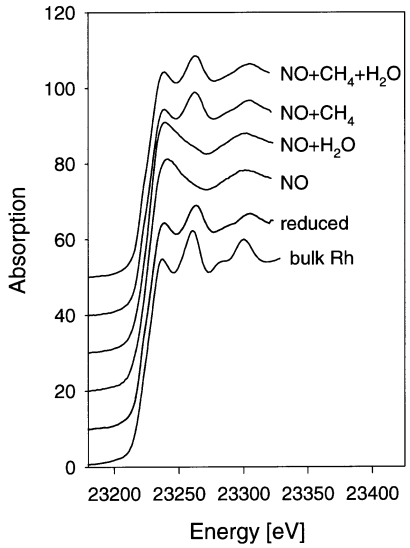

Figure 5. XANES of Rh/MCM-41 after reduction, after adsorption of NO, after co-adsorption of NO and CH_4 with and without H_2O and of bulk Rh.

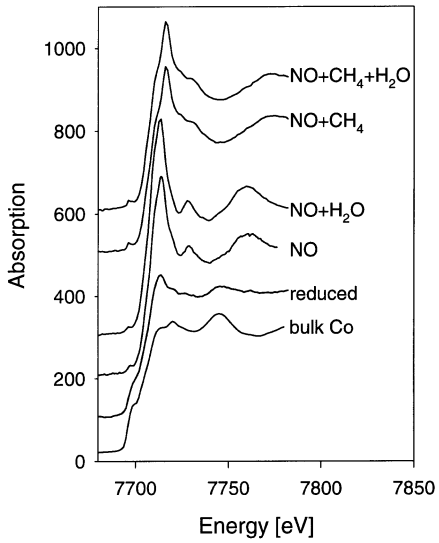

Figure 7. XANES of Co/MCM-41 after reduction, after adsorption of NO, after co-adsorption of NO and CH_4 with and without H_2O and of bulk Co.

centrations of unreduced species or to the interaction of the small metal clusters with the walls of the molecular sieve [21]. However, these changes are only a minor effect compared with the changes in the XANES after adsorption of the reactants.

The XANES of Rh/MCM-41 after exposure to the mixture of all reaction gases, i.e., after adding 10 vol% O_2 into the reaction gas mixture, are shown in figure 8. For all samples the increase of the peak above the absorption edge indicated an oxidation of the metal. Moreover, the oxidation state was identical when water was pre-adsorbed on the catalyst or when the water vapor was added as the last component into the carrier gas.

Note that in the X-ray absorption spectroscopy experiments for Pt only the L_{III}-absorption edge (11564 eV) was accessible, while for Co and Rh K-absorption edges (7709 and 23220 eV) could be investigated. Conceptually, the L_{III}-edge results from transitions from the $p_{3/2}$ state into unoccupied $s_{1/2}$, $d_{3/2}$ and $d_{5/2}$ states and the K-edge from transition from s into p states. Most reduced transition metals already exhibit a strong peak above their L_{III}-edges, while on K-edges of reduced metals this peak is usually not present [22]. Therefore, the changes in the XANES were much more

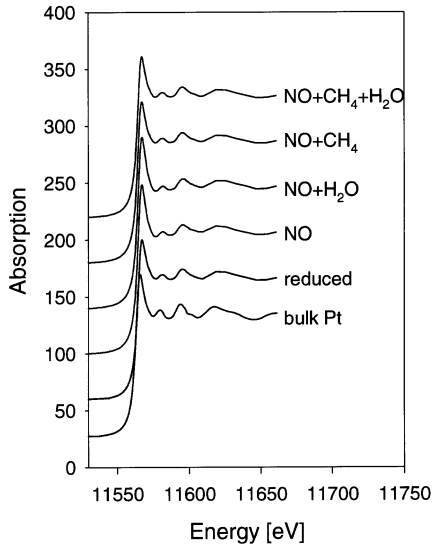

Figure 6. XANES of Pt/MCM-41 after reduction, after adsorption of NO, after co-adsorption of NO and CH_4 with and without H_2O and of bulk Pt.

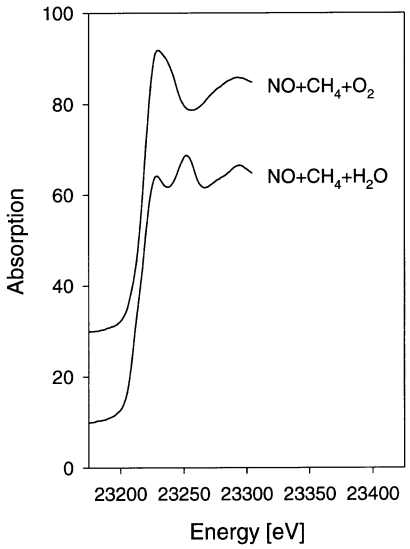

Figure 8. XANES of Rh/MCM-41 after exposure to all reaction gases.

pronounced on the Co and Rh K-absorption edges than on the Pt L_{III}-edge.

4. Discussion

Exposure to 3000 ppm NO at 673 K led to an oxidation of all samples investigated. On Rh/MCM-41 and Pt/MCM-41 the presence of water vapor strongly decreased the time needed to reach the new oxidation state, but did not lead to a different level of oxidation compared to the exposure of the catalysts with NO only. This indicates that on these catalysts water is not blocking sorption sites during the reaction and that an intermediate complex between NO and water was formed, which facilitates the oxidation of the metallic species.

Co/MCM-41 was oxidized by the presence of water in the carrier gas stream by the following reaction:

$$Co + H_2O \rightarrow CoO + H_2$$

Note that the equilibrium of this reaction is almost completely on the right-hand side when water vapor is present [23]. On Co/MCM-41 the co-adsorption of H_2O and NO led to a higher oxidation level of the metal compared to the adsorption of NO only. For Co/MCM-41 the role of H_2O is entirely different compared to the other two catalysts investigated. Metallic Co is thermodynamically not stable in the presence of water vapor and, therefore, the Co/MCM-41 sample was rapidly oxidized during the co-adsorption of H_2O and NO.

CH_4 acts as a reducing agent under the reaction conditions. Even in the presence of NO Rh/MCM-41 and Pt/MCM-41 were reduced when CH_4 was added into the carrier gas. Water did not have any influence on the reduction of these two samples by CH_4. Co/MCM-41 was only partially reduced by the presence of CH_4; however, the fully reduced metallic state of Co could not be reached. After adding O_2 into the reaction gas mixture all catalysts were oxidized and the resulting oxidation state was independent of the presence of water vapor. It is interesting to note that the addition of water vapor as first or as last component into the mixture of the reaction gases did not lead to a different chemistry on the metal surface.

Therefore, we would like to speculate that the decrease of activity during the catalytic reduction of NO over these catalysts caused by water vapor results from the interaction between water and the reactants. When water is present under reaction conditions the metal surface is still accessible for NO. For the noble metal catalysts the presence of water facilitates the partial oxidation of the metal surface, but did not lead to an additional oxidation of the metal. For Co/MCM-41 the presence of water vapor caused an oxidation of the metallic component, however, the oxidation state of Co was the same when oxygen was present in the carrier gas.

5. Conclusions

Transition metal containing MCM-41 catalysts showed significant changes in the oxidation state of the metal during co-adsorption of NO, CH_4 and O_2. The presence of NO led to an oxidation of the catalysts. For the noble metal containing MCM-41 catalysts a complete reduction of the metal clusters was observed during the co-adsorption of NO and CH_4, while Co/MCM-41 was only partially reduced under these conditions. All catalysts were oxidized when O_2 was added into the gas mixture. The presence of water vapor did not influence the oxidation state of the noble metal containing MCM-41 catalysts, but led to an increased rate of the oxidation in NO atmosphere, while Co/MCM-41 catalyst was already fully oxidized by the presence of water vapor at reaction temperature.

The influence of water on the metal sites in molecular sieves depends on the type of the metal. For precious metals, water forms an intermediate with the other reaction gases, which facilitates the oxidation of the metal clusters, while for non precious metals, e.g., Co, it influences directly the oxidation state of the metal clusters.

Acknowledgement

The work was supported by the "Fonds zur Förderung der Wissenschaftlichen Forschung" under project FWF P10874. We would like to thank the CLRC Daresbury Laboratory for the provision of synchrotron radiation under the EEC contract number CHGE-CT93-0036. We would like to thank S. Feast and H. Bitter (University of Twente) for their help during the experiments at the SRS.

References

[1] J.H. Armor, Appl. Catal. B 1 (1992) 221.
[2] H. Bosch and F. Janssen, Catal. Today 2 (1988) 369.
[3] M. Iwamoto and H. Hamada, Catal. Today 10 (1991) 57.
[4] M. Iwamoto, Catal. Today 29 (1996) 29.
[5] Y. Li and K.W. Hall, J. Catal. 129 (1991) 202.
[6] H. Hirabayashi, H. Yahiro, N. Mizuno and M. Iwamoto, Chem. Lett. (1992) 2235.
[7] Y. Li, P.J. Battavio and J. Armor, J. Catal. 142 (1993) 561.
[8] X. Feng and W.K. Hall, J. Catal. 166 (1997) 368.
[9] D.J. Liu and H. Robota, Catal. Lett. 21 (1993) 291.
[10] C. Marquez-Alvarez, I. Rodriguez-Ramos, A. Guerre-Ruiz, G.L. Haller and M. Fernandez-Garcia, J. Am. Chem. Soc. 119 (1997) 2905.
[11] J.S. Beck, J.C. Vartuli, W.J. Roth, M.E. Leonowicz, C.T. Kresge, K.D. Schmitt, C.T.W. Chu, D.H. Olson, E.W. Sheppard, S.B. McCullen, J.B. Higgins and J.L. Schlenker, J. Am. Chem. Soc. 114 (1992) 10834.
[12] M. Nomura, in: *Series on Synchrotron Radiation Techniques and Applications*, Vol. 2, ed. Y. Iwasawa (1996) p. 93.
[13] W.H. McMasters, N.K.D. Grande, J.H. Mallet and J.H. Hubell, *Compilations of X-Ray Cross Sections* (Lawrence Radiation Laboratory, 1969).

[14] B.J. McHugh, G.L. Larsen and G.L. Haller, J. Phys. Chem. 94 (1990) 8621.
[15] D.A. Outka and J. Stöhr, J. Chem. Phys. 88 (1988) 3539.
[16] D.C. Koningsberger and R. Prins, *Principles, Applications, Techniques of EXAFS, SEXAFS and XANES*, Chemical Analysis, Vol. 92 (Wiley, New York, 1988).
[17] K. Asakura, in: *Series on Synchrotron Radiation Techniques and Applications*, Vol. 2, ed. Y. Iwasawa (1996) p. 34.
[18] R.E. Benfield, J. Chem. Soc. Faraday Trans. 88 (1992) 1107.
[19] M. Englisch, J.A. Lercher and G.L. Haller, in: *Series on Synchrotron Radiation Techniques and Applications*, Vol. 2, ed. Y. Iwasawa (1996) p. 276.
[20] A. Jentys, A. Lugstein and H. Vinek, Zeolites, accepted (1997).
[21] M. Vaarkamp, B.L. Mojet, M.J. Kappers, J.T. Miller and D.C. Koningsberger, J. Phys. Chem. 99 (1995) 16067.
[22] G. Meitzner, G.H.Via, F.W. Lytle and J.H. Sinfelt, J. Phys. Chem. 96 (1992) 4960.
[23] D.R. Lide, ed., *Handbook of Chemistry and Physics*, 75th Ed. (CRC Press, Boca Raton, 1995).